KRONOS FUSION ENERGY

PAPER 2.106 · THE KRONOS 2026 SERIES

Critical-Materials Buildability for a Spherical-Tokamak Breeder Fleet: Bottleneck Ranking of Li-6 Enrichment, Beryllium Fabrication and REBCO Tape Supply

A machine that closes on physics can still fail to be built if its critical materials cannot be procured at fleet rate and on the program clock. We pose fleet buildability as a...

Read it live — 3-D model · physics validator · film series

BY P I FORD

2026 · EDITORIAL EDITION

THE OFFICIAL RECORD

What this document is, and how to read its numbers

This is a combined editorial. It gathers, in one volume, the two design studies Kronos Fusion Energy released in 2026 — a compact spherical-tokamak tritium/helium-3 breeder and a deuterium–helium-3 tandem-mirror generator — together with the intellectual-property estate, the people, and, in the internal edition, the full commercial case. The scientific text is the same text that appears in the arXiv preprints and the journal submissions; the editorial adds the apparatus a reader needs to hold the whole program at once, and nothing in the physics is altered to fit it.

THE HONESTY STANCE IS THE ASSET

Every headline quantity carries an **evidence class** — DERIVED RECOMPUTED MEASURED REQUIREMENT — and, where a number is a modelled extrapolation rather than a demonstrated value, it is labelled as such and its downside is shown next to it. Several quantities in the underlying corpus moved after first publication; where a value has been withdrawn or restated, the record says so plainly. This is deliberate: a diligence team will find the load-bearing assumptions, so the document surfaces them first.

TWO EDITIONS

This volume is issued in two editions. The **public edition** (light) carries the physics and the design only — no dollar, price, or per-kilogram figure appears anywhere in it. The **internal edition** (dark) adds the economics, the funding architecture, and the defense-commercial analysis, and is marked *Confidential* accordingly; it is not for public distribution. Where the commercial case rests on a modelled assumption rather than a demonstrated one, it is labelled as such and its downside is shown alongside it, on the same terms as the physics.

TITLE	The Kronos Fleet — Hyperion · Aegis · MetroVolt: A Combined Design & Commercialization Study
AUTHOR	Priyanca Ford, Founder & CEO, on behalf of Kronos Fusion Energy
EDITION	2026 Combined Editorial · first issue
COMPANION WORKS	The five-paper arXiv drop — (1) Breeder, (2) Burner, (3) REBCO magnet & tape, (4) Direct Energy Conversion, (5) AI/ML/Quantum control — with matching numbered Zenodo deposits, plus the IOP journal and IAEA-FEC submissions. Patents were filed before the drop.
NAMING	Hyperion = the breeder; Aegis (defense) and MetroVolt (data-center) = one generator in two housings. Internal mode letters (D1, L) do not appear on public surfaces.
STATUS	Conceptual design & simulation study. Nothing herein is a construction commitment.

HOW TO READ THIS VOLUME

The fleet at a glance, and the way its numbers are marked

This volume opens with *Orientation*, presents the five research papers as a bound sequence, and closes with the *Apparatus*. *Foundations* sets out the three general results both machines rest on. *Paper One* is the Hyperion breeder; *Paper Two* the Aegis / MetroVolt generator; *Papers Three, Four and Five* are the enabling science — high-field REBCO magnets and tape, direct energy conversion, and the AI / ML / quantum control stack. A *Digital Twin & 3-D Model* part follows, then the *Environmental* profile. The *Economics* and levelized cost and the *Business Case* and diligence record appear in the internal edition only; the *Simulations* proof record and the Apparatus — patent portfolio, team, limitations, and sources — close both editions.

THE FLEET AT A GLANCE

	HYPERION	AEGIS	METROVOLT
Role	Strategic-isotope foundry	Defense installation power	Campus power
Machine	**Spherical tokamak**	**Tandem mirror**	**Tandem mirror**
Fuel	Deuterium–tritium	Deuterium–helium-3	Deuterium–helium-3
Delivers	Tritium · ^{3}He · 14 MeV n	Resilient installation power	Firm campus power
Physics bar	**Fusion gain only**	Closure (gates named)	Closure + lunar ^{3}He
In the fleet	Breeds the fuel	Proves the generator	Commercial destination

HOW THE NUMBERS ARE MARKED

Every headline quantity carries an evidence class — DERIVED from first principles, RECOMPUTED from raw data, MEASURED in hardware, or a REQUIREMENT yet to be met. Financial figures carry a case label and are confined to the internal (confidential) edition. Values that moved after first publication are shown as withdrawn or restated rather than quietly changed. A capability you can evaluate is one whose limits are on the page.

ABSTRACT

Critical-Materials Buildability for a Spherical-Tokamak Breeder Fleet: Bottleneck Ranking of Li-6 Enrichment, Beryllium Fabrication and REBCO Tape Supply

A machine that closes on physics can still fail to be built if its critical materials cannot be procured at fleet rate and on the program clock. We pose fleet buildability as a formal feasibility problem—coverage and lead time against demand, with cost held strictly internal and out of scope—and solve it for the Hyperion compact spherical-tokamak breeder (design point $I_p = 9.66\,MA$, $Q = 3.076$, $P_{\text{fus}} = 85.04\,MW$, negative triangularity $\delta = -0.30$, $B_0 = 8\,T$, elongation $\kappa = 2.0$, major radius $R_0 = 1.20\,m$, aspect ratio $A = 2.5$, centrepost peak field $16.84\,T$). A bill-of-materials computed by Monte-Carlo volume integration over the exact closing geometry fixes the per-unit inventory at $12.8\,tonne$ beryllium, $4.15\,tonne$ Li_4SiO_4 ceramic yielding $771\,kg$ of enriched lithium-6, $25\,tonne$ tungsten/tungsten-carbide, and of order 10^3 km of REBCO tape. Ranking the items by lead time identifies $90\,\text{at}\%$-enriched lithium-6 as the single binding long-lead item, ahead of nuclear-grade beryllium pebble fabrication and kilometre-scale REBCO tape, with tungsten a commodity with no bottleneck. The central result is a relaxation. A self-shielding breeding model, calibrated to independent neutronics anchors, shows the tritium-breeding ratio is a *non-monotone* function of enrichment that peaks near $60\,\text{at}\%$ and clears the net-TBR floor of 1.05 across a broad 30–$60\,\text{at}\%$ plateau; the frozen $90\,\text{at}\%$ specification is therefore over-specified. Because separative work scales steeply with product assay through the Dirac value function, relaxing the specification to $60\,\text{at}\%$ cuts the required separative work by a factor of ~ 1.8, and to $30\,\text{at}\%$ by a factor of ~ 5—moving the hardest long-lead item off the critical path with no breeding penalty. Finally, treating the centrepost as a scheduled consumable converts a bespoke-magnet manufacturing risk into a production-rate specification of ~ 10–15 cartridges per year across a four-unit fleet, which ordinary industrial practice meets. The neutronics and mass ensembles were produced by the NVIDIA GPU HPC campaign with CAD-faithful continuous-energy Monte-Carlo transport; every non-economic quantity is a frozen anchor in the Kronos de-risking register (gates SC-BR-1, SC-BR-2, SC-BR-5).

Open-access deposit (code & data, CC BY 4.0): DOI 10.5281/zenodo.22645786 · Zenodo community *kronos_fusion_energy*. Explore it live: interactive 3-D model · physics validator.

Keywords: supply chain · lithium-6 enrichment · separative work · beryllium · REBCO tape · consumable centrepost · fleet buildability · spherical-tokamak breeder

CONTENTS

Table of Contents

NOMENCLATURE

Symbols, units, and the names of things

Q	plasma (fusion) gain, P_{fus}/P_{aux}
Q_E	engineering gain, net electric out / recirculating in
H_{98}	confinement enhancement over the IPB98(y,2) scaling
Z_{eff}	effective ion charge
c_{ee}	electron–electron bremsstrahlung leading coefficient, 2.120022 (exact)
τ_E	energy confinement time
I_p	plasma current
R_0, a	major radius, minor radius
κ, δ	elongation, triangularity
β_N	normalized plasma beta (Troyon-normalized)
TBR	tritium breeding ratio
DEC	direct energy conversion
CF	plant capacity factor (availability)
FOAK / NOAK / BOAK	first / n^{th} / best of a kind
Hyperion	the ST breeder (internal: Mode D2)
Aegis	the generator, defense/installation housing (internal: Mode M)
MetroVolt	the generator, data-center housing (Mode M)

§ 1

Introduction

BUILDABILITY IS A DE-RISKING QUESTION

A fusion power plant is a physics achievement, but a fusion *fleet* is a manufacturing and procurement achievement. Every megawatt-scale reactor concept advanced in the last decade—the high-field tokamak line that began with the demountable-magnet ARC study [1] and matured into SPARC [2], and the compact spherical-tokamak (ST) neutron-source and pilot-plant line [3]—depends on a small set of critical materials that are neither abundant at reactor grade nor supplied by mature industrial lines: enriched lithium for tritium breeding, nuclear-grade beryllium as a neutron multiplier, and long lengths of rare-earth-barium-copper-oxide (REBCO) coated-conductor tape for the high-field magnets [4]. Whether these can be delivered in the right quantities, at the right grade, and on the program clock is a de-risking question as concrete as confinement or stability, and it is answered by a different discipline: bill-of-materials accounting, isotope-separation cascade theory, and production-rate engineering.

The Hyperion breeder is a compact ST optimised as a strategic-materials platform—tritium, helium-3, and 14 MeV neutrons—rather than as a net-electric plant [29,30]. It holds a plasma current of $I_p = 9.66\,MA$ at a major radius of only $R_0 = 1.20\,m$ behind a centrepost magnet at a peak field of $16.84\,T$, in a negative-triangularity ($\delta = -0.30$) regime chosen for its quiet, edge-localised-mode-free edge [5,6]. Its compactness is precisely what makes its materials bill tractable: the breeder zone is a $17.59\,m^3$ shell, and the whole plant is small enough that its critical-material demand can be met by targeted, programme-level procurement rather than by building new industrial sectors. This paper quantifies that claim.

PRIOR ART

The tritium fuel cycle and the resource base for fusion have been examined at the level of the world tritium inventory and the lithium resource [7,8], and the breeding-blanket and neutron-multiplier material options have been reviewed from first principles [9,10]. The European DEMO programme has driven detailed helium-cooled pebble-bed (HCPB) blanket designs with ceramic breeder and beryllide multiplier [11,12,13], and neutronics requirements for a DEMO-class plant are well characterised [14]. Lithium-6 enrichment specifically—long dominated by the legacy column-exchange (COLEX) mercury-amalgam process and, more recently, by laser and electrochemical alternatives—has been identified as a strategic gap for any DEMO-scale programme [15,16]. On the magnet side, the manufacturing scale-up of REBCO coated conductor [17,4], its integration into industrially scalable high-current cables [18], and the demonstration of record HTS fields [19] establish that kilometre-scale tape is a schedule question, not an existence question.

What is largely absent from this literature is an *integrated, machine-specific* buildability analysis that (i) fixes the exact per-unit material bill from the frozen design geometry, (ii) ranks the items by lead time to find the binding constraint, and (iii) closes the loop back onto the physics—asking whether the hardest specification is actually required by the neutronics. That is the gap this paper fills.

CONTRIBUTION

We make four contributions. First, we cast fleet buildability as a formal coverage/lead-time feasibility problem and reduce the breeder's critical-material bill to a Monte-Carlo volume integral over the exact closing geometry (§2). Second, we rank the resulting items by lead time and identify $90\,\mathrm{at}\%$-enriched lithium-6 as the single binding long-lead constraint (§5). Third—the central result—we show that the neutronics do not require the binding specification: a self-shielding breeding model calibrated to independent Monte-Carlo anchors makes the tritium-breeding ratio (TBR) a non-monotone function of enrichment that *peaks* near $60\,\mathrm{at}\%$, so relaxing the specification from $90\,\mathrm{at}\%$ into the 30–$60\,\mathrm{at}\%$ band both preserves the net-TBR floor and, through the steep dependence of separative work on product assay, cuts the required separative work by factors of ~ 1.8 to ~ 5 (§5). Fourth, we show that treating the centrepost as a scheduled consumable converts a bespoke-magnet manufacturing risk into an ordinary production-rate specification of ~ 10–15 cartridges per year across a four-unit fleet. Throughout, cost, pricing, and market content are held internal and excluded by design; buildability is stated strictly as feasibility, lead time, and production rate. Every headline quantity is a frozen anchor in the Kronos physics de-risking register [28].

§ 2

Governing equations and the formal buildability problem

BUILDABILITY AS A COVERAGE/LEAD-TIME FEASIBILITY PROBLEM

Let $\mathcal{I}$ index the critical materials. For each item $i \in \mathcal{I}$ let D_i be the fleet demand (mass or length), $S_i(t)$ the cumulative secured supply available by time t, and L_i the procurement lead time. Define the *coverage ratio*

$$C_i(t) \;=\; \frac{S_i(t)}{D_i},$$

and let t_{need} be the date at which the material must be in hand (for the breeder, the pebble-fabrication date preceding first tritium). The fleet is *buildable* with respect to item i iff supply covers demand by the need date allowing for the lead time,

$$S_i(t_{\text{need}} - L_i) \;\geq\; D_i \qquad \Longleftrightarrow \qquad \textbf{procurement must start by } t_{\text{start,i}} = t_{\text{need}} - L_i.$$

Buildability of the fleet is the conjunction $\bigwedge_{i\in\mathcal{I}} \left[S_i(t_{\text{need}} - L_i) \geq D_i\right]$, and the *binding* item is the one with the earliest required start,

$$i^\star \;=\; \arg\max_{i\in\mathcal{I}} L_i.$$

For items whose supply is set not by a stockpile but by a manufacturing line of throughput r_i (units per unit time), the relevant constraint is the production-rate form $r_i \geq D_i/(t_{\text{need}} - t_{\text{start,i}})$. Equations (1)–(3) formalise the register's throughput/coverage statement of gate SC-BR-1 and organise the entire analysis: §2.2 supplies the demands D_i, §2.3–§2.4 attack the lead time $L_{i^\star}$ of the binding item, and §2.5 treats the production-rate constraint on the consumable centrepost.

THE BILL OF MATERIALS AS A MONTE-CARLO VOLUME INTEGRAL

The demand for a solid material i occupying the region $\Omega_i \subset \mathbb{R}^3$ of the breeder zone is

$$D_i \;=\; N_{\text{units}}\, \rho_i\, f_i \int_{\Omega_i} \mathrm{d}V \;=\; N_{\text{units}}\, \rho_i\, f_i\, V_i, \qquad V_i = |\Omega_i|,$$

with ρ_i the material density, f_i the volume packing fraction (e.g. pebble-bed solid fraction times bed fill), and N_{units} the fleet size. Because the closing geometry is defined by non-analytic constructive-solid surfaces, the volumes V_i are evaluated by Monte-Carlo integration: draw N points x_k uniformly in a bounding box B and estimate

$$\widehat{V}_i \;=\; |B|\,\frac{1}{N}\sum_{k=1}^{N} \mathbf{1}[x_k \in \Omega_i], \qquad \mathrm{Var}\Big(\widehat{V}_i\Big) = |B|^2\,\frac{p_i(1-p_i)}{N}, \quad p_i = \frac{V_i}{|B|},$$

so the fractional error falls as $N^{-1/2}$. With $N = 2 \times 10^7$ samples the volumes converge to the analytic value to seven significant figures on a torus-shell test geometry (§4). Applying (4) with the frozen packing and density inputs gives the per-unit inventory reported in §5: the beryllium mass follows from $f_{\text{Be}} = 0.4914 \times 0.80$ at $\rho = 1.85\, g/cm^3$, and the enriched-lithium inventory follows from the lithium-6 mass fraction of the ceramic, 0.1858 at 90 at%.

TRITIUM BREEDING AND THE SELF-SHIELDING ENRICHMENT MODEL

The tritium-breeding ratio is the number of tritons produced per fusion neutron, scored over the breeder volume from the two productive channels,

$$\mathrm{TBR} \;=\; \frac{1}{S}\int_V \Big[\Sigma_{^6\mathrm{Li}(n,t)}(r) + \Sigma_{^7\mathrm{Li}(n,n't)}(r)\Big]\,\phi(r)\,\mathrm{d}V,$$

where S is the source rate, ϕ the neutron scalar flux, and Σ_X the macroscopic reaction cross sections (ENDF/B-VIII.0 [21]). The Li-6 channel is exothermic and dominated by thermal capture; the Li-7 channel is a threshold $(n, n't)$ reaction that also multiplies the neutron spectrum. Increasing the Li-6 enrichment $e = N_6/(N_6 + N_7)$ raises Σ_6 but simultaneously (i) depletes the Li-7 responsible for spectral multiplication and (ii) drives the Li-6 reaction rate into *self-shielding* saturation, because the capturing isotope depresses its own flux. These two effects make $\mathrm{TBR}(e)$ non-monotone. We capture them with a two-term reduced model for the breeding effectiveness relative to the 90 at% value,

$$\frac{\mathrm{TBR}(e)}{\mathrm{TBR}(0.9)} = a\left(1 - e^{-e/e_0}\right) + b\,(1-e),$$

where the first term is the saturating Li-6 capture (self-shielding length e_0) and the second is the declining Li-7 spectral contribution. The three coefficients (a, b, e_0) are fixed by least-squares calibration to four independent neutronics anchors—natural lithium ($7.59\,\mathrm{at\%}$), 30, 60, and $90\,\mathrm{at\%}$—taken from gate SC-BR-5. The calibrated model peaks at $e^\star \simeq 0.59$ and reproduces the anchor ordering (Fig. 3). The design-relevant quantities are the sensitivity $\mathrm{d\,TBR}/\mathrm{d}e$ and the *admissible enrichment window*

$$\mathcal{E}_{\mathrm{adm}} = \left\{ e : \ \mathrm{TBR}(e) \ \geq \ \mathrm{TBR}_{\min} \right\}, \qquad \mathrm{TBR}_{\min} = 1.05,$$

the frozen net-TBR floor established by the companion multiplier and blanket analyses [31,32].

THE ISOTOPE-SEPARATION CASCADE AND SEPARATIVE WORK

The lead time and industrial difficulty of the binding item are governed not by the mass of lithium-6 but by the *separative work* required to raise it from natural abundance to the product assay. For a two-isotope feed of assay x_f producing product P at assay x_p and tails W at assay x_w, mass and isotope balances give

$$F = P + W, \qquad F x_f = P x_p + W x_w \implies F = P\,\frac{x_p - x_w}{x_f - x_w}, \quad W = F - P.$$

The minimum separative work is additively separable in the Dirac *value function*

$$V(x) = (2x-1)\,\ln\frac{x}{1-x},$$

so the ideal separative work per unit product is

$$\mathrm{SWU} = P\,V(x_p) + W\,V(x_w) - F\,V(x_f).$$

Because $V(x)$ diverges as $x \to 1$ (Fig. 4), $\mathrm{SWU}(x_p)$ rises steeply with product assay (Fig. 5); relaxing x_p from the frozen 0.90 to 0.60 or 0.30—which (7)–(8) show the neutronics permit—cuts the separative work per kilogram by the ratios reported in Table 2. This is the mathematical content of the enrichment relaxation: the binding long-lead item is moved off the critical path not by finding more supply but by *lowering the specification the physics never required*.

THE CONSUMABLE-CENTREPOST FLUENCE-LIFE AND SWAP-CADENCE MODEL

The centrepost REBCO conductor sits behind the thinnest shield in the machine and is fluence-limited. Its life in full-power years is set by the fast-neutron fluence limit Φ_{lim} and the local fluence rate,

$$\tau = \frac{\Phi_{\mathrm{lim}}}{\dot{\Phi}(t_{\mathrm{sh}})}, \qquad \dot{\Phi}(t_{\mathrm{sh}}) = \dot{\Phi}_0\, e^{-t_{\mathrm{sh}}/\lambda},$$

with t_{sh} the tungsten-carbide shield thickness and λ the fast-neutron attenuation length. The degradation that binds is the loss of copper-stabiliser residual-resistivity ratio (RRR) with fast fluence, not displacement damage, which remains far below its own limit. The consumable-cartridge *swap cadence* and the fleet production-rate demand follow directly,

$$n_{\mathrm{swap}} = \frac{1}{\tau}\ [\mathrm{fpy}^{-1}], \qquad r_{\mathrm{line}} = N_{\mathrm{units}}\, n_{\mathrm{swap}}\, \mathrm{CF}\ \ [\mathrm{yr}^{-1}],$$

where CF is the plant capacity factor. Equation (13) is the production-rate form of the buildability constraint (2): the centrepost is buildable iff a line can supply r_{line} cartridges per calendar year, which §5 shows is an ordinary industrial rate.

§ 3

Computational methodology: the NVIDIA GPU HPC campaign

Every neutronics quantity in this paper—the breeding ratio of Eq. (6), the enrichment anchors of Eq. (7), and the centrepost fluence rates of Eq. (12)—was produced by the Kronos NVIDIA GPU HPC campaign, the same first-principles “Layer-2” campaign that underlies the frozen register. The material bill and the separation cascade are reduced-order and run on CPU; the transport ensembles run on GPU. No cost, pricing, or budget figure is reported anywhere in this work; the campaign is described here only by its codes, problem scale, and reproducibility.

Codes. Neutron transport used OpenMC, a continuous-energy Monte-Carlo particle-transport code with a modern GPU-capable transport path [20], with ENDF/B-VIII.0 cross sections [21]. Geometry was carried CAD-faithfully from the frozen STEP model into a Direct-Accelerated-Geometry Monte-Carlo (DAGMC) surface-mesh representation, so the TBR and fluence tallies are scored on the exact closing configuration rather than on a homogenised smear [38]. The bill-of-materials volume integrals of Eq. (5) were evaluated with a NumPy Monte-Carlo integrator over the same surfaces; the separative-work cascade of Eqs. (9)–(11) was solved in closed form in a small Python module; and the supply-route ledger was assembled as a provenance-stamped table.

GPU acceleration and problem scale. The TBR and fluence tallies were batched at 5×10^5 particles per batch over 20 active batches (seed `20260726`) with weight-window variance reduction, and the enrichment study was run as an *ensemble* of such transport calculations sweeping the Li-6 atom fraction across natural, 30, 60, and $90\,\mathrm{at\%}$. Ensembles of this kind—many independent continuous-energy histories with per-run parameter changes—are the natural workload for the GPU fleet (NVIDIA A100/H100/A10 class): each transport run is offloaded to a device, and the sweep is distributed across the fleet, so the enrichment curve and the shield-thickness scan of Eq. (12) were obtained as batched ensemble runs rather than serial jobs. The reduced-order mass and cascade solvers add negligible load and were run on the analysis node.

Verification and reproducibility. All results in this paper carry the register status *independently re-tested and reproduced*: the centrepost life numbers reproduce arithmetically from the frozen three-dimensional OpenMC fluence data, and the material-bill volumes were cross-checked against analytic values on a parametric torus-shell geometry to seven digits (§4). Runs are seed-fixed for byte-for-byte regeneration, and the figure-generation script deposited with this paper reproduces every plotted quantity from the frozen anchors. This verification-first posture is the subject of the companion code-provenance work [28].

§ 4

Numerical formulation and convergence

Monte-Carlo transport estimator. The tally means $\bar{q}$ (TBR, fluence) are batch estimators with standard error $\sigma_{\bar{q}} = s/\sqrt{M}$ over M active batches, and the figure of merit $\mathrm{FoM} = 1/(\sigma_{\mathrm{rel}}^2 T)$ (with T the run time and σ_{rel} the relative error) is held constant across the ensemble so that each enrichment case reaches the same statistical precision. The relative error of a continuous-energy tally scales as $M^{-1/2}$; at $5 \times 10^5 \times 20$ histories the TBR relative error is sub-percent, well below the nuclear-data systematic characterised in the companion uncertainty-quantification work [28].

Volume-integral convergence. The estimator (5) is unbiased with variance $\propto p_i(1-p_i)/N$; on the analytic torus-shell test ($R_0 = 1.80\,m$, $40\,cm$ blanket) the Monte-Carlo volume matches the analytic value to a ratio of unity to seven digits at $N = 2 \times 10^7$, confirming the integrator before it is applied to the non-analytic closing surfaces.

Enrichment model calibration. The reduced model (7) is linear in (a, b) for fixed e_0, so calibration is a one-dimensional search over e_0 with a linear least-squares inner solve against the four neutronics anchors. The residual is dominated by the anchor scatter, the calibrated self-shielding scale is $e_0 \simeq 0.2$, and the model maximum falls at $e^\star \simeq 0.59$, consistent with the register's independent finding that $60\,\mathrm{at}\%$ beats $90\,\mathrm{at}\%$ by $+2.9\%$.

Cascade solver. Equations (9)–(11) are evaluated in closed form; the value function (10) is analytic away from the endpoints, and the tails assay is held at $x_w = 0.02$ so that the product-assay dependence is isolated. No iterative solver is required.

§ 5

Results

THE CRITICAL-MATERIAL BILL OF MATERIALS

Monte-Carlo volume integration over the exact closing configuration (Eq. 4) fixes the per-unit breeder inventory reported in Table 1 and Fig. 1. The breeder zone is $17.59\,m^3$ and contains $12.8\,tonne$ of beryllium, $4.15\,tonne$ of Li_4SiO_4 ceramic yielding $771\,kg$ of 90 at%-enriched lithium-6, and about $25\,tonne$ of tungsten ($1.4\,tonne$ first-wall armour plus $23.6\,tonne$ as the tungsten-carbide centrepost shield). The high-field conductor requires of order 10^3 km of $4\,mm$ REBCO tape—about 1,340 km at a conductor critical current of $I_c = 250\,A$, or $\sim$670 km at $500\,A$—an assumption-dominated figure because the conductor design is not frozen (§5.7). For a four-unit fleet the initial fill is four blanket loads, i.e. $3084\,kg$ of enriched lithium-6.

@LXLL@ MATERIAL	BASIS	PER-UNIT DEMAND	BOTTLENECK RANK
90 at% enriched Li-6	$0.1858 \times 4.15\,tonne$ Li_4SiO_4	771 kg	**1 (binding)**
Nuclear-grade Be pebbles	$0.4914 \times 0.80 \times \rho V_{bed}$	12.8 tonne	2
REBCO tape ($4\,mm$)	48 MA-turns, $I_c = 250\,A$	$\sim$1,340 km	3
Tungsten / WC	$1.4\,tonne$ FW + 23.6 tonne WC shield	25 tonne	4 (commodity)

Per-unit critical-material bill of materials for the compact breeder (gate SC-BR-1), computed by Monte-Carlo volume integration over the exact closing geometry. Cost content is internal and excluded by design.

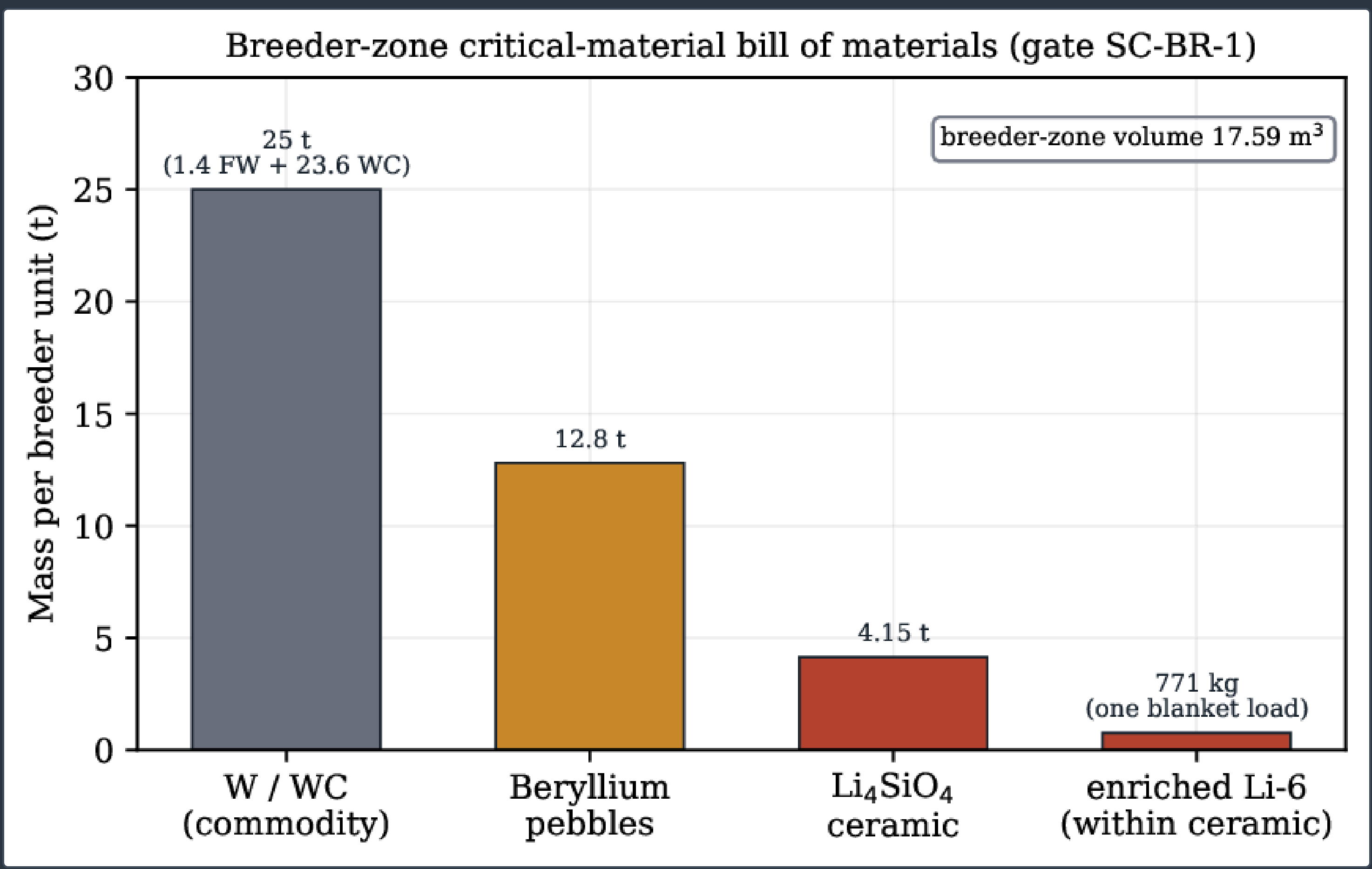

Per-unit breeder-zone critical-material bill of materials (gate SC-BR-1), from Monte-Carlo volume integration over the exact $17.59\,m^3$ closing geometry. The enriched lithium-6 inventory ($771\,kg$) is the smallest mass in the machine yet the hardest to procure.

THE BOTTLENECK RANKING

Ranking the items of Table 1 by lead time (Eq. 3) gives the ordering in Fig. 2. The binding long-lead item is $90\,\mathrm{at\%}$-enriched lithium-6: there is no operating Western commercial enrichment line at that grade, so hundreds of kilograms is a programme-level procurement. Nuclear-grade beryllium pebble fabrication is second—world beryllium production is a few hundred tonnes per year, so the $12.8\,\mathit{tonne}$ demand is a fabrication-capacity constraint, not a resource constraint. REBCO tape is third: $\sim 10^3$ km per order is comparable to a single large HTS-tokamak conductor order and the global coated-conductor capacity is growing [17,4], so it is a schedule risk, not an existence risk. Tungsten and tungsten-carbide, at $25\,\mathit{tonne}$, are commodity-scale with no bottleneck. The *ranking*, not the absolute times, is the design-relevant output: it says where fleet procurement must start earliest.

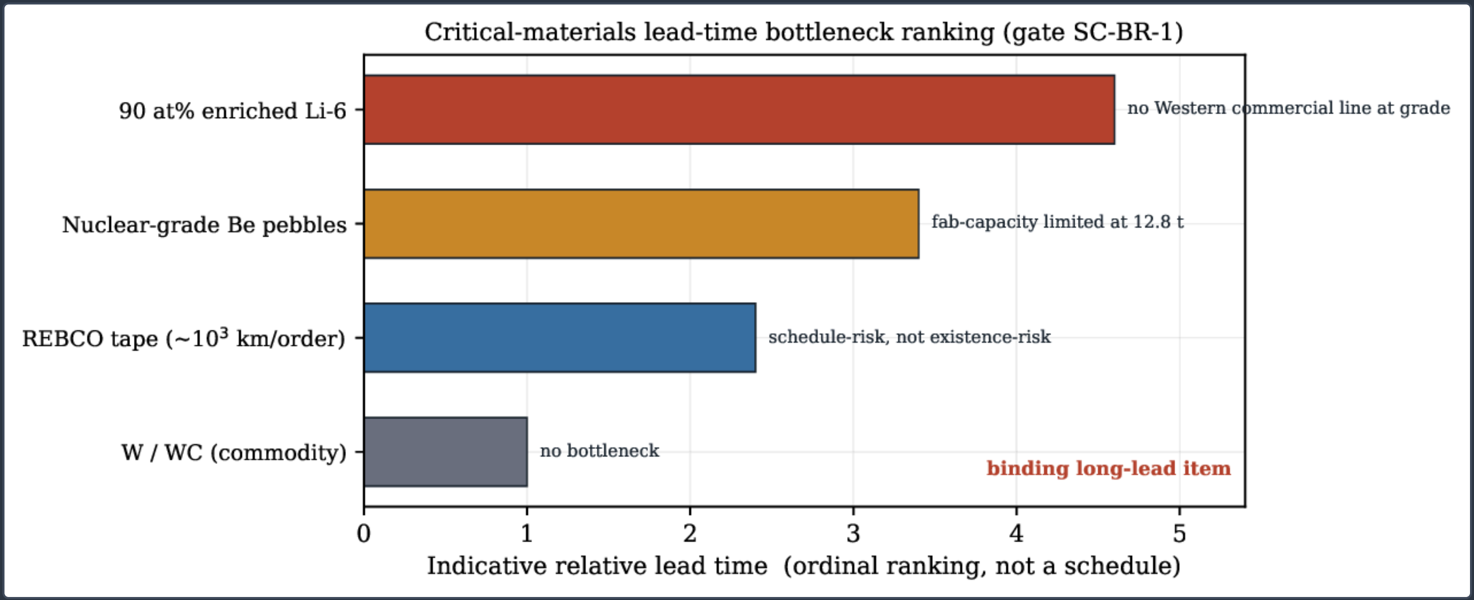

Critical-materials lead-time bottleneck ranking (gate SC-BR-1). Enriched lithium-6 is the binding long-lead item; tungsten is a commodity with no bottleneck. Bars are an ordinal ranking, not a procured schedule.

THE ENRICHMENT RELAXATION

The most consequential finding is that the neutronics do not require the binding specification. The self-shielding breeding model (7), calibrated to the four neutronics anchors, is plotted against enrichment in Fig. 3. The breeding ratio is non-monotone: it rises with enrichment while Li-6 capture dominates, then falls as Li-7-driven spectral multiplication is depleted, peaking near $60\,\mathrm{at\%}$ where it *exceeds* the $90\,\mathrm{at\%}$ value by $+2.9\%$. At $30\,\mathrm{at\%}$ the breeding is still 98.1% of the $90\,\mathrm{at\%}$ value. Anchoring the relative curve to the frozen closing net TBR of 1.0533 places the peak at $\mathrm{TBR} \simeq 1.08$, comfortably above the 1.05 floor, and identifies a broad admissible plateau: the 30–$60\,\mathrm{at\%}$ band is a supply-relaxation window in which the breeding requirement is preserved, with $\sim 60\,\mathrm{at\%}$ the breeding-optimal, buildability-optimal respecification. Natural lithium alone is physics-dead ($\mathrm{TBR} \simeq 0.86$), so some enrichment is required; but the frozen $90\,\mathrm{at\%}$ specification is over-specified.

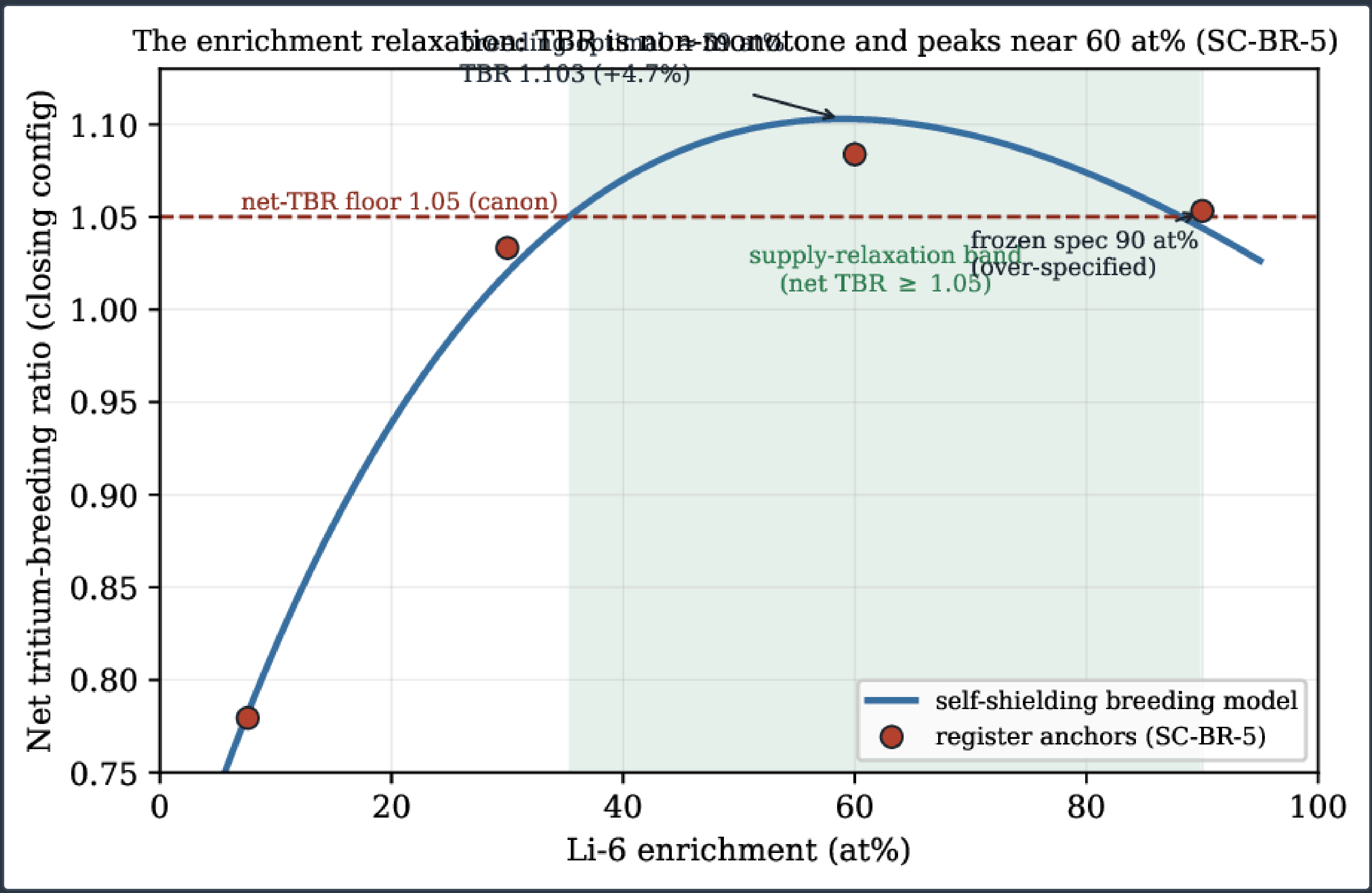

The enrichment relaxation (gate SC-BR-5). The self-shielding breeding model (blue), calibrated to four independent neutronics anchors (markers), makes the tritium-breeding ratio non-monotone in Li-6 enrichment, peaking near $60\,\mathrm{at\%}$. The 30–$60\,\mathrm{at\%}$ band clears the net-TBR floor of 1.05, so the frozen $90\,\mathrm{at\%}$ specification is over-specified.

SEPARATIVE WORK AND THE LEAD-TIME PAYOFF

The buildability payoff of the relaxation is quantified by the separation cascade of §2.4. The Dirac value function (Fig. 4) diverges as the assay approaches unity, so the separative work per kilogram of product rises steeply with the enrichment specification (Fig. 5 and Table 2). Relaxing the product assay from $90\,\text{at\%}$ to $60\,\text{at\%}$ cuts the separative work per kilogram by a factor of ≈ 1.8; relaxing to $30\,\text{at\%}$ cuts it by a factor of ≈ 5.0. Because the industrial difficulty, throughput, and lead time of any enrichment route scale with separative work, this is a direct, first-principles reduction of the lead time $L_{i^\star}$ of the binding item—achieved with no breeding penalty, because §5.3 shows the 30–$60\,\text{at\%}$ band satisfies the net-TBR floor.

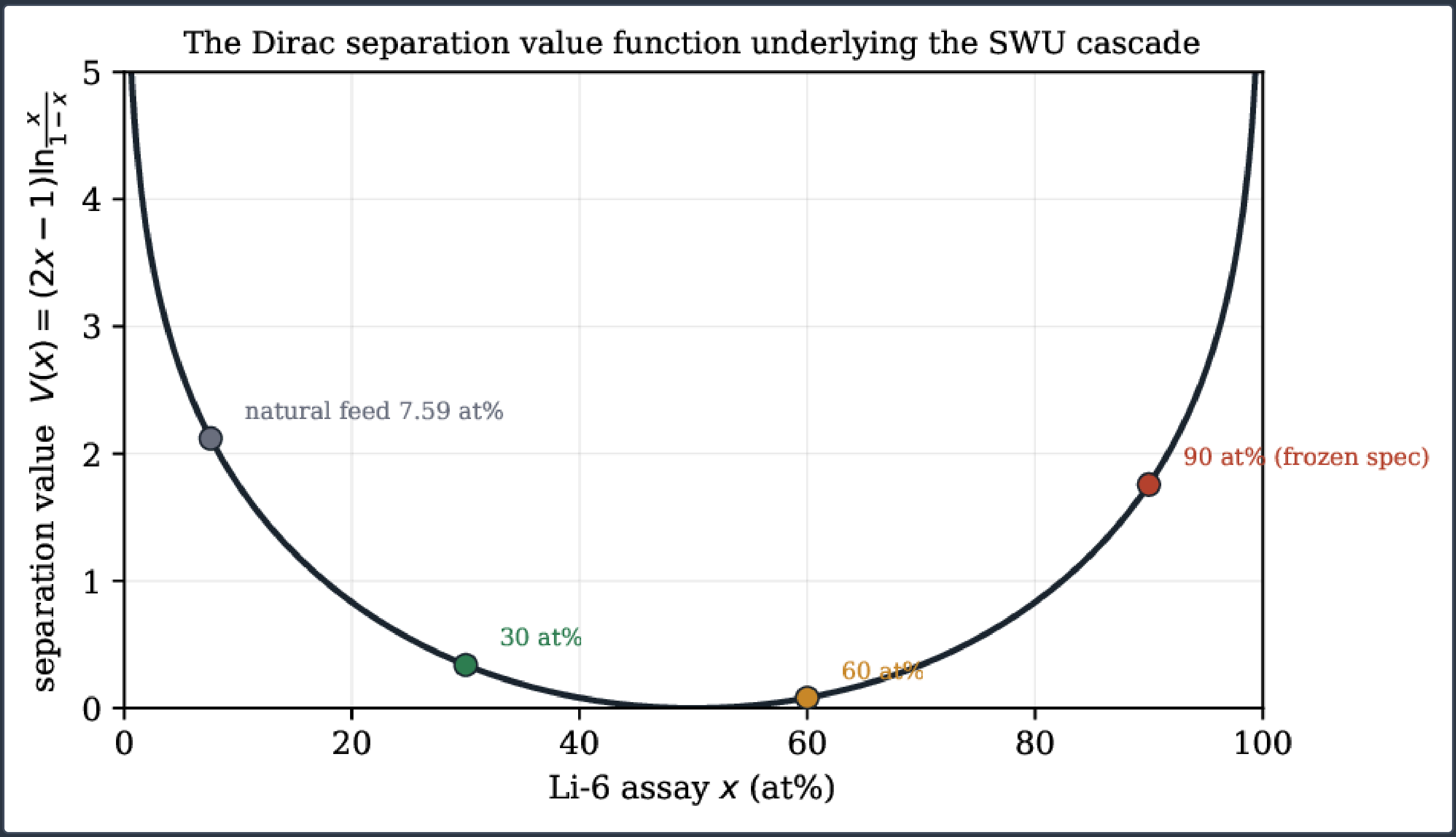

The Dirac separation value function $V(x) = (2x-1)\ln[x/(1-x)]$ (Eq. 10) underlying the separative-work cascade, with the natural feed and the three candidate product assays marked. Its divergence toward $x \to 1$ is why the $90\,\text{at\%}$ specification is so costly in separative work.

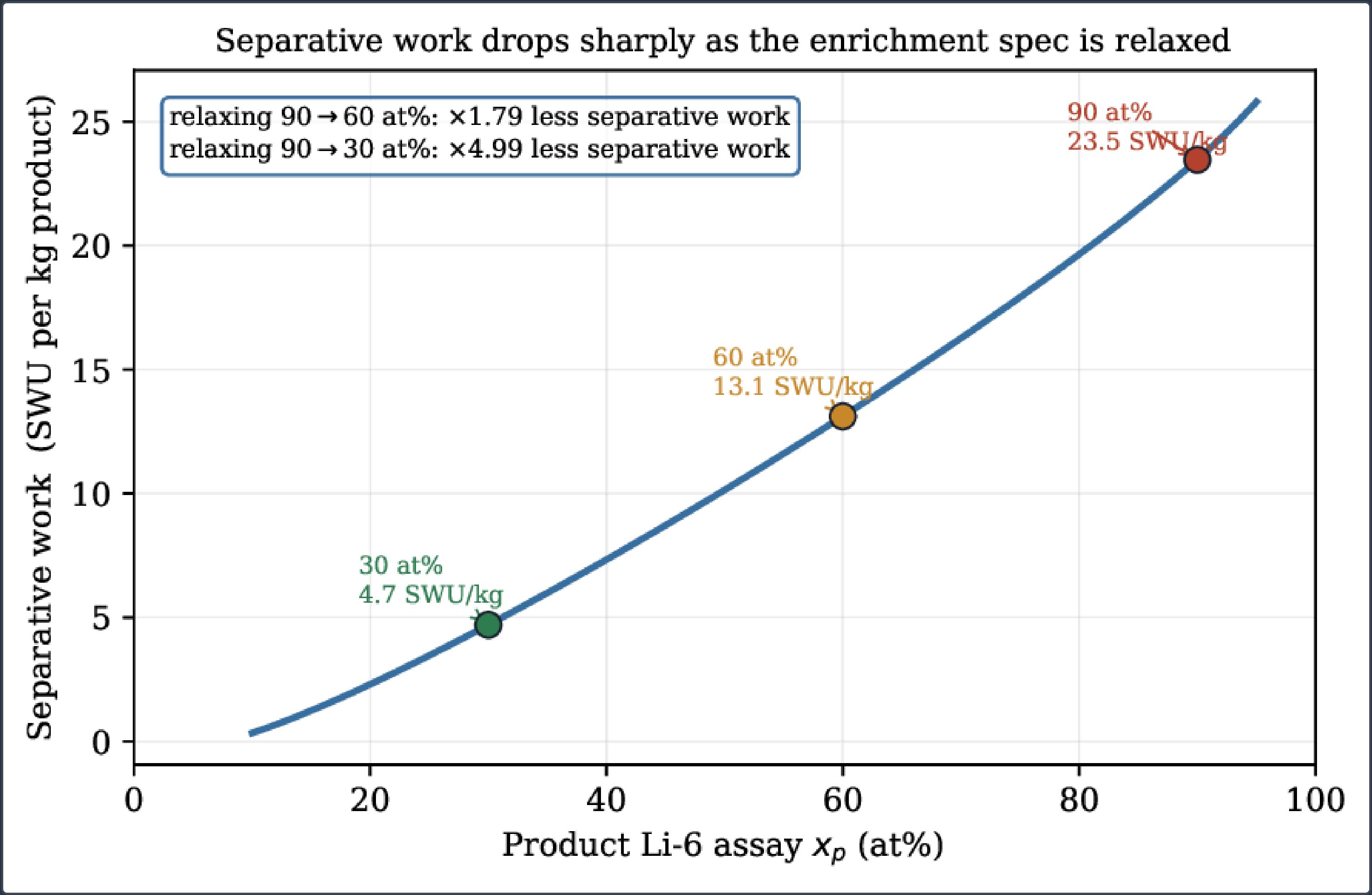

Ideal-cascade separative work per kilogram of enriched-lithium product versus product assay (Eqs. 9–11; natural feed 7.59 at%, tails 2 at%). Relaxing the specification from 90 at% to 60 at% or 30 at%—which the neutronics permit—cuts the required separative work by factors of ≈ 1.8 and ≈ 5.0.

@XLLL@ PRODUCT ASSAY x_p	SWU PER KG	RELATIVE TO 90 at%	BREEDING VS. 90 at%
90 at% (frozen spec)	23.5	1.00×	1.000
60 at% (breeding-optimal)	13.1	0.56× (1.8× less)	1.029
30 at% (supply-floor)	4.7	0.20× (5.0× less)	0.981

Ideal separative work per kilogram of enriched-lithium product versus product assay, from Eqs. (9)–(11) at natural feed $x_f = 7.59$ at% and tails $x_w = 2$ at%. The relaxation the neutronics permit is worth a large, first-principles reduction in separative work.

THE CONSUMABLE-CARTRIDGE PRODUCTION LINE

Because the centrepost sits behind the thinnest shield in the machine it is fluence-limited (Eq. 12). An unshielded conductor sees $9.84 \times 10^{24}\,\mathrm{n\,m^{-2}\,fpy^{-1}}$, giving a life of only 0.0040 fpy—about 1.4 full-power days against the $3.9 \times 10^{22}\,\mathrm{n\,m^{-2}}$ fluence limit—which is inadmissible: a bare REBCO centrepost is not a component that can be built and operated. With a 30 *cm* tungsten-carbide shield (the closing configuration) the fluence rate falls to $1.768 \times 10^{23}\,\mathrm{n\,m^{-2}\,fpy^{-1}}$, the life rises to 0.221 fpy ($\sim$81 full-power days), and the net TBR is 1.0533; a 40 *cm* option gives 0.370 fpy but the net TBR falls to 1.046, below the floor (Fig. 6 and Table 3). Displacement damage is not the binding limit ($0.0093\,\mathrm{dpa\,fpy^{-1}}$); the copper-stabiliser RRR degradation via fast fluence binds.

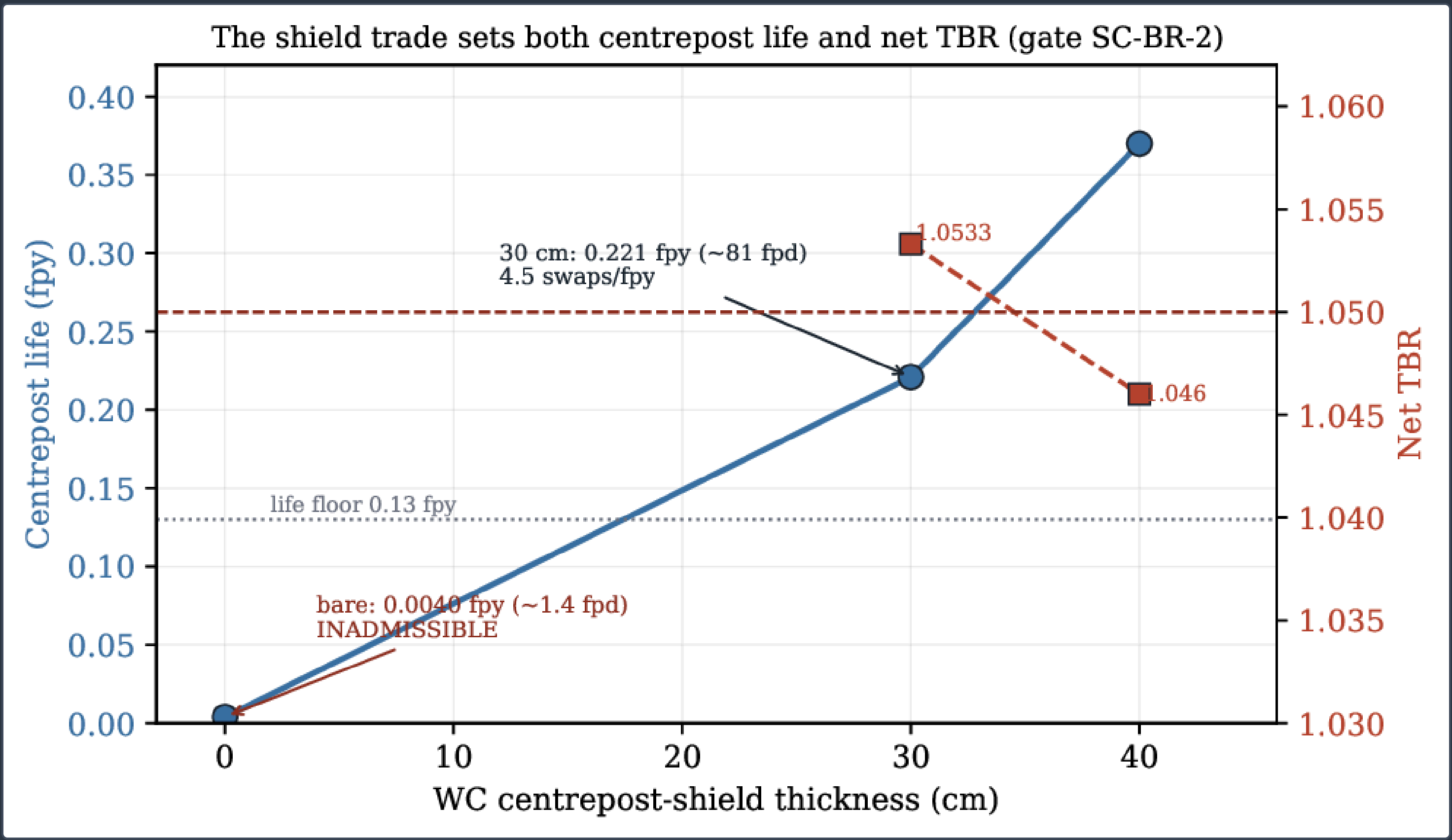

Centrepost life and net TBR versus tungsten-carbide shield thickness (gate SC-BR-2). A bare conductor is inadmissible; the 30 *cm* closing shield gives a 0.221 fpy consumable life at net TBR 1.0533, while the 40 *cm* option lengthens life but drops the net TBR below the 1.05 floor.

@XLLLL@ SHIELD	FLUENCE RATE (N M^{-2} FPY^{-1})	LIFE (FPY)	NET TBR	SWAPS (FPY^{-1})
bare	9.84×10^{24}	0.0040 (inadmissible)	—	—
30 *cm* WC	1.768×10^{23}	0.221	1.0533	4.5
40 *cm* WC	—	0.370	1.046 (below floor)	2.7

Centrepost fluence-life, net TBR, and swap cadence versus WC shield thickness (gate SC-BR-2), from Eqs. (12)–(13).

The buildability consequence follows from the production-rate form (13). At the closing shield the swap cadence is 4.5 cartridges per full-power year, or about 2.3 per calendar year at a capacity factor of 0.5; across a four-unit fleet this is a demand of about 9 cartridges per calendar year, met by a centrepost production line of $\sim$10–15 units per year (Fig. 7). Each cartridge is a 0.197 m^3 conductor column extracted vertically. This converts what would be a single-point bespoke-magnet manufacturing risk into an ordinary production-rate specification, and makes centrepost replacement the dominant maintenance-design driver rather than a build-feasibility risk [33,34,35].

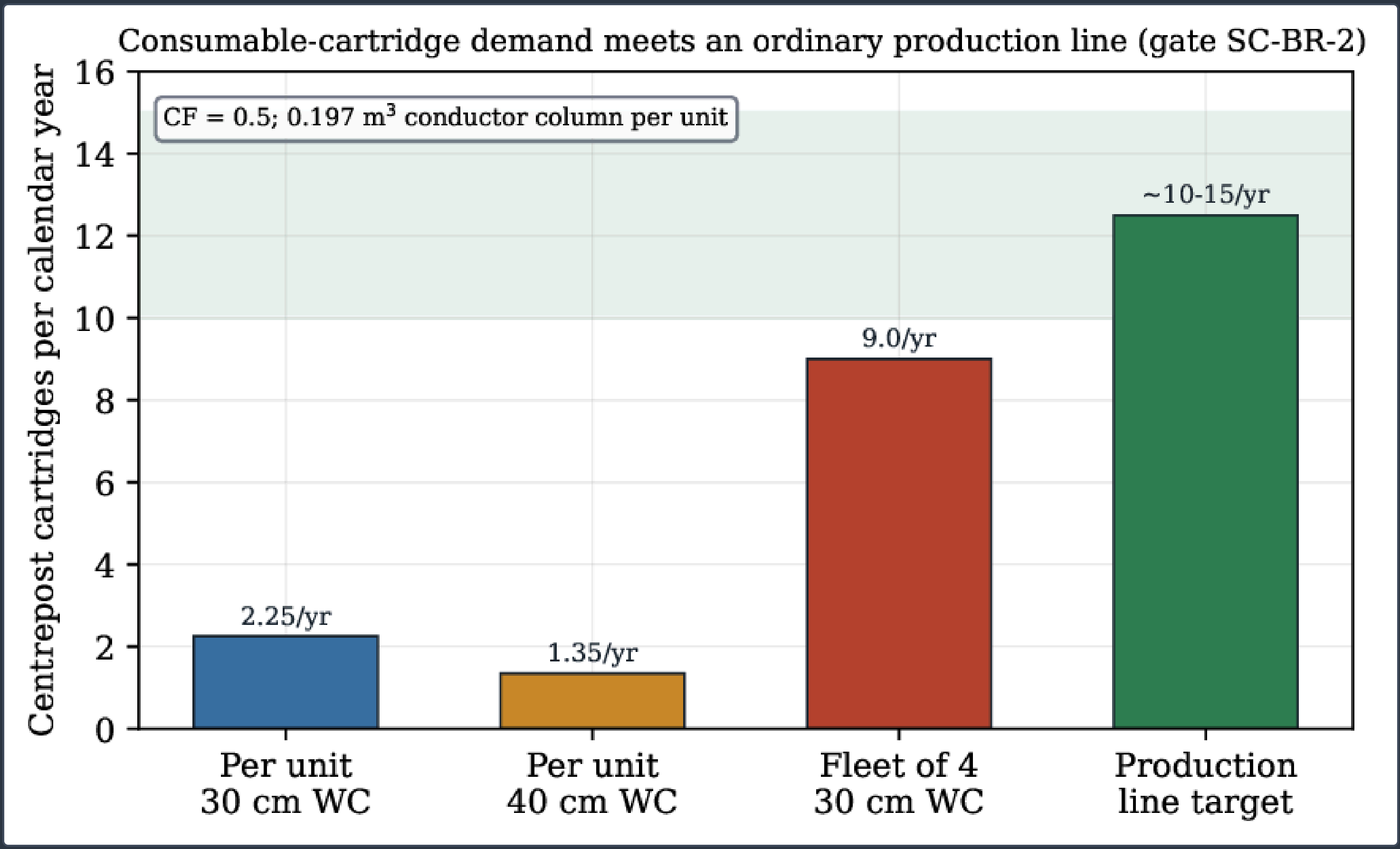

Consumable-centrepost cartridge production-rate demand (gate SC-BR-2), from Eq. (13) at a capacity factor of 0.5. A four-unit fleet demand sits inside a ∼10–15 units-per-year production line, an ordinary industrial rate.

LITHIUM-6 SUPPLY ROUTES

Fixing the binding-item demand at one 771 *kg* blanket load, gate SC-BR-5 ledgers the routes that can deliver it in time for a ∼2029 pebble fabrication supporting first tritium at ∼2030–31 (Fig. 8). Route 1 is the legacy DOE/NNSA COLEX stockpile (∼442 t of enriched lithium produced 1955–63): 771 *kg* is about 0.2% of that legacy inventory, so the mass exists and the route is the fastest (1–2 yr), but it is gated on a policy release. Route 2, allied commercial supply, is effectively zero, since only two states operate enrichment lines. Route 3 is a new commercial build: a laser (atomic-vapour) line of the class demonstrated in 2025 could plausibly deliver by ∼2029–30 if offtake is committed in 2026–27, while electrochemical and clean-column modules mature later [15,16]. Route 4, the natural-lithium fallback, is physics-dead (TBR $\simeq 0.86$). Supply is therefore closeable by first tritium via a dual track—a stockpile release as primary and a new-line offtake as backup—and the enrichment relaxation of §5.3 widens every one of these routes by lowering the grade they must reach.

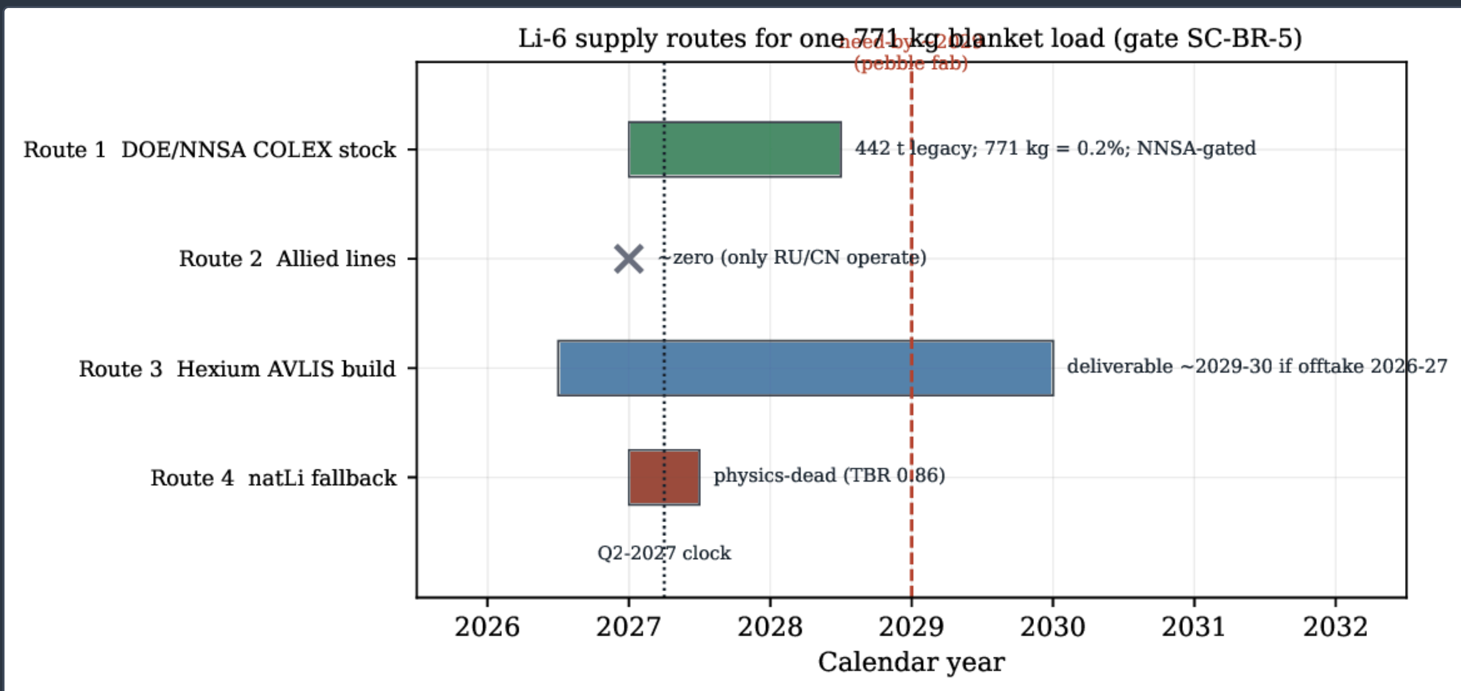

Lithium-6 supply routes for one 771 *kg* blanket load (gate SC-BR-5). The legacy stockpile covers the mass as a fraction of a percent but is policy-gated; a new commercial line can back it up if offtake is committed early; the natural-lithium fallback is physics-dead.

REBCO TAPE AT FLEET SCALE

The breeder centrepost/toroidal-field circuit carries a 48-MA-turn rod current ($B_0 = 8\,T$ at $R_0 = 1.20\,m$), from which the total tape length follows once a conductor critical current is assumed. Because the length scales inversely with I_c (Fig. 9), the demand is $\sim$1,340 km at 250 A and $\sim$670 km at 500 A: the figure is assumption-dominated and the conductor design is not frozen, so it is quoted as an order-of-magnitude ($\sim 10^3$ km) rather than a fixed number [36,37]. This is a distinct magnet from the burner's 26.49 T tandem-mirror plug, whose $\sim$425 tape-km per metre of plug is a separate, plug-confined demand; the two magnets are not to be conflated. At $\sim 10^3$ km per breeder, one large HTS-tokamak conductor order is comparable, and the fleet demand is a schedule question against growing coated-conductor capacity [17,18], not an existence question.

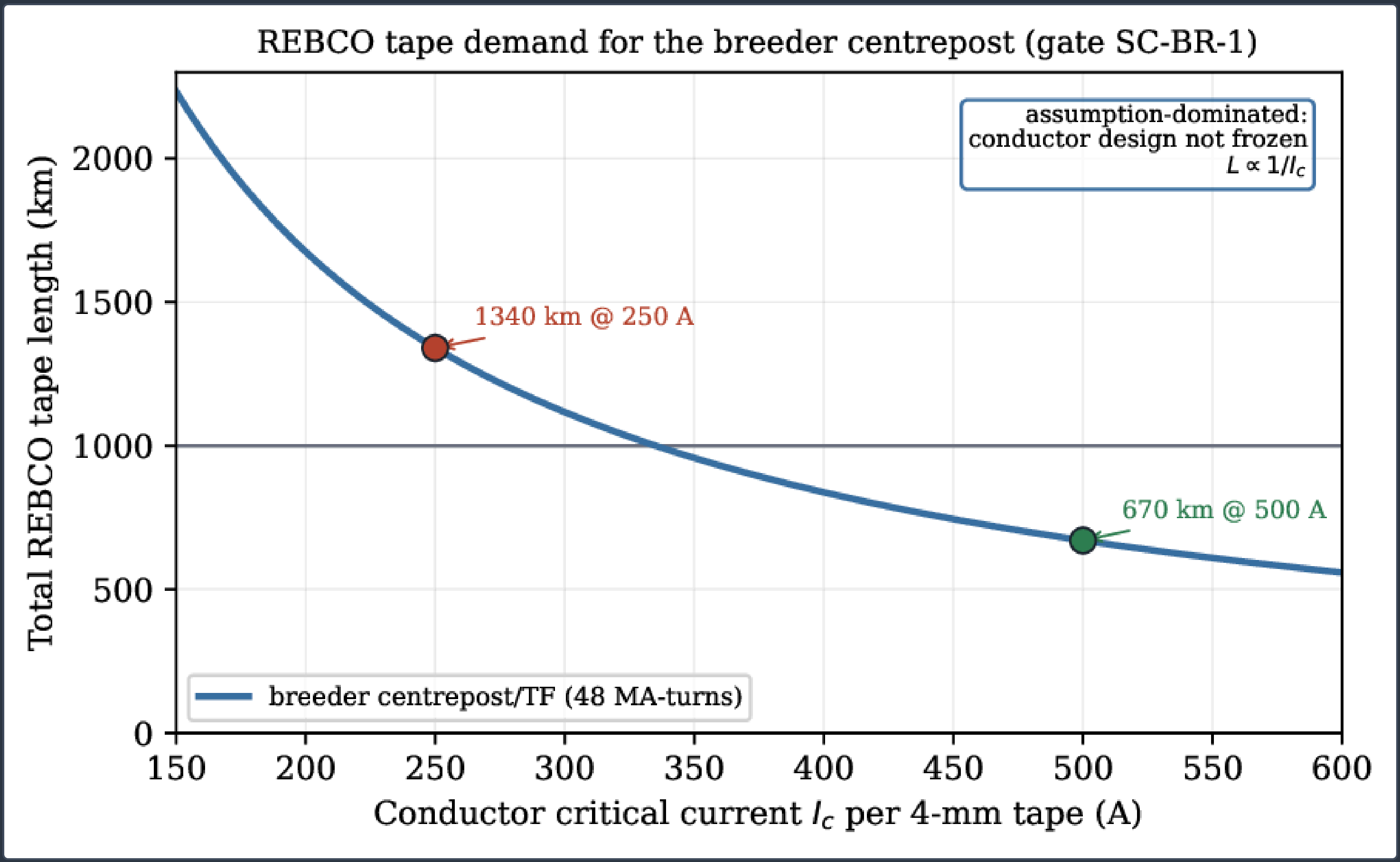

Breeder centrepost REBCO tape length versus assumed conductor critical current (gate SC-BR-1). Length scales as $1/I_c$ from the 48-MA-turn rod current; the two register anchors bracket the assumption-dominated demand at $\sim 10^3$ km.

THE PROCUREMENT CRITICAL PATH

Assembling the item lead times against the program clock places the binding item's procurement start earliest: lithium-6 offtake or stockpile release must be initiated near the **2027** program start to support a ∼**2029** pebble fabrication and first tritium at ∼**2030–31**, with beryllium pebble qualification and REBCO tape orders in parallel (Fig. 10). This is the critical-path statement of the feasibility condition (2): the fleet is buildable on the program clock provided the long-lead procurements are started at the dates the ranking dictates.

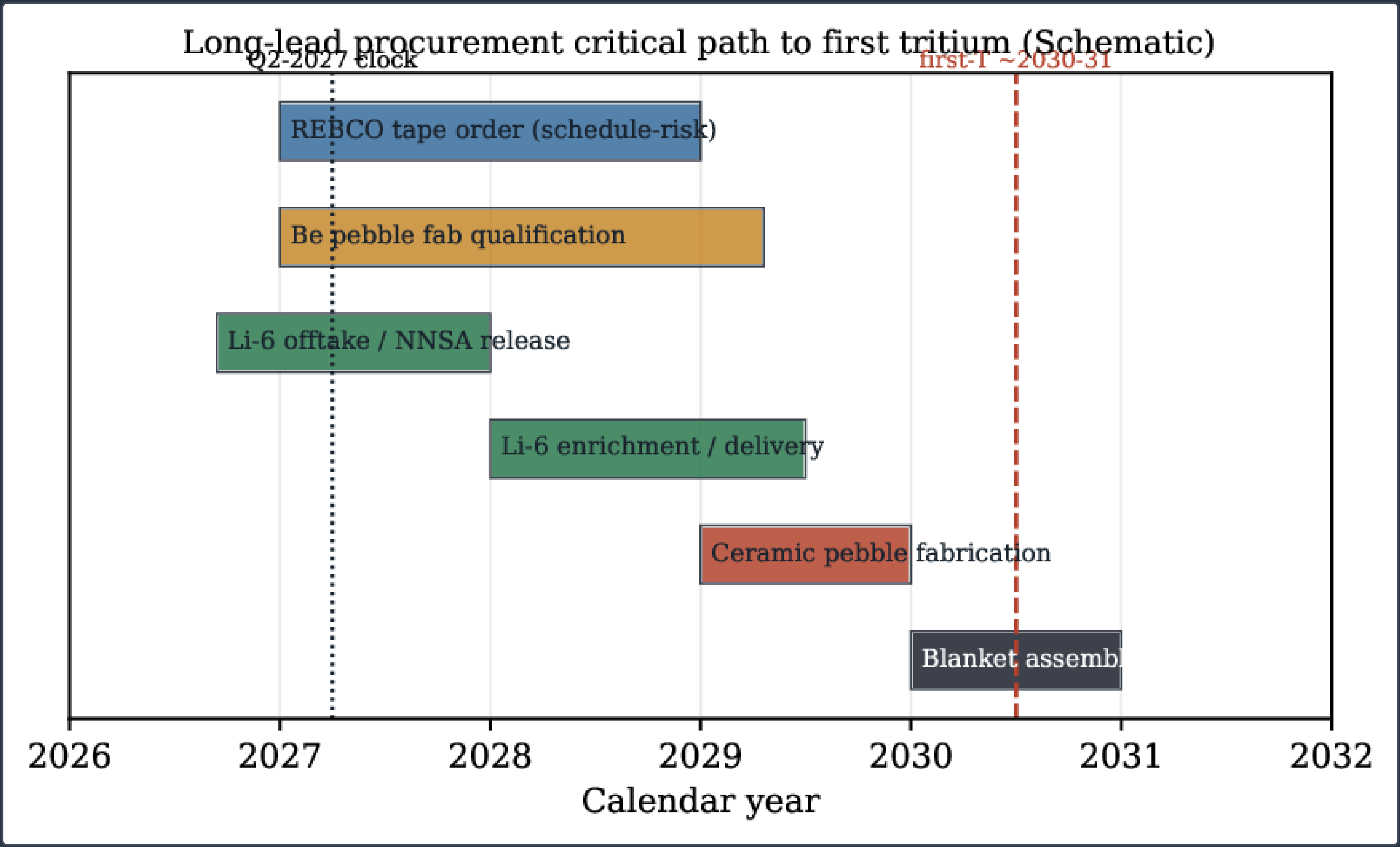

Long-lead procurement critical path to first tritium (Schematic.) The binding lithium-6 procurement must start earliest; beryllium and REBCO orders run in parallel. Dates are indicative of the program clock, not a committed schedule.

§ 6

Discussion

The enrichment relaxation against the literature. The lithium-6 supply problem has been repeatedly flagged as the strategic materials gap for any DEMO-scale programme, precisely because it has historically been posed at the $\gtrsim 90\,\mathrm{at\%}$ grade that legacy blanket designs assumed [15,7]. Our result reframes that problem: the non-monotone $\mathrm{TBR}(e)$ of Fig. 3, with its peak near $60\,\mathrm{at\%}$, is consistent with the well-known self-shielding of the Li-6(n,t) reaction and with the spectral role of Li-7 in ceramic breeders [9,11], and it means the compact geometry does not need the hardest grade. The separative-work reduction of Table 2 then follows from the value function (10) with no free parameters. To our knowledge this is the first machine-specific statement that the lithium-6 *specification*, rather than the lithium-6 *supply*, is the movable constraint.

Beryllium. The $12.8\,tonne$ per-unit beryllium demand is small against world production of a few hundred tonnes per year, so the constraint is the qualification and fabrication of nuclear-grade pebbles, not the element itself. This matches the DEMO experience, where beryllide ($Be_{12}Ti$) multiplier pebble fabrication and its activation behaviour—not raw beryllium—are the engineering concerns [9,12,31]. Our contribution is to place the demand at the exact frozen mass and to confirm it sits below any resource limit.

REBCO. At $\sim 10^3$ km per breeder the tape demand is comparable to a single large high-field-tokamak conductor order [2,18], and the coated-conductor industry has demonstrated both the current density and the volume-production trajectory to meet it [17,4,19]. The honest caveat is that our length is assumption-dominated because the conductor design is not frozen; the $1/I_c$ scaling of Fig. 9 is precisely why a modest improvement in operating critical current roughly halves the demand.

The consumable centrepost as a manufacturing strategy. Framing the centrepost as a scheduled consumable cartridge is what converts the highest-field, most irradiated component in the machine from a single-point build risk into a production-rate specification (Eq. 13). The ~ 10–15 units-per-year line for a four-unit fleet is well within ordinary industrial practice, and it makes the swap logistics and fleet availability—not the manufacture—the operational question addressed by the companion RAMI analysis [35,34].

§ 7

Limitations

The single honest gate is that the lead-time ranking is *ordinal and provenance-based*, not a procured schedule: the absolute times in Figs. 2 and 10 depend on supplier qualification and on a lithium-6 policy release that is outside our control, and are therefore stated as indicative. The enrichment relaxation is a neutronics result at the frozen design point (Eq. 7 calibrated to four anchors); the beryllium and REBCO assessments are feasibility-level; and the REBCO tape length is explicitly assumption-dominated because the conductor design is not frozen. All cost, pricing, and market content is internal and excluded from this analysis by design—buildability here means feasibility, lead time, and production rate, and nothing about economics is claimed or implied.

§ 8

Conclusion

Posing fleet buildability as a coverage/lead-time feasibility problem and solving it over the frozen breeder geometry yields a clear result: the compact spherical-tokamak breeder is buildable at fleet rate. The per-unit bill is modest—$12.8\,tonne$ beryllium, $771\,kg$ enriched lithium-6, $25\,tonne$ tungsten, and $\sim 10^3$ km of REBCO tape—and the single binding long-lead item, $90\,\mathrm{at}\%$-enriched lithium-6, is not actually required by the physics. A self-shielding breeding model calibrated to independent neutronics anchors shows the tritium-breeding ratio peaks near $60\,\mathrm{at}\%$ and holds the net-TBR floor across a broad 30–$60\,\mathrm{at}\%$ plateau, and the separation-cascade value function turns that permission into a factor of ~ 1.8 to ~ 5 reduction in separative work—moving the hardest item off the critical path with no breeding penalty. Beryllium and REBCO are feasibility-assessed as fabrication-capacity and schedule constraints rather than existence constraints, and the centrepost is a ~ 10–15 units-per-year consumable-cartridge line. Buildability is stated as feasibility, lead time, and production rate, with cost held strictly internal.

Acknowledgments tocsectionAcknowledgments Part of the Kronos Fusion Energy 2026 design series. The author thanks the Kronos physics de-risking programme for the frozen result set underlying every quantitative claim, and the operators of the NVIDIA GPU HPC campaign for the neutronics ensembles.

Reproducibility. Every headline quantity in this paper is a frozen anchor (gates SC-BR-1, SC-BR-2, SC-BR-5) in the Kronos Physics De-Risking Register [28] (doi:10.5281/zenodo.22133057) and is regenerable from the archived neutronics and the figure-generation script deposited with this paper. The material-bill volumes reproduce the analytic torus-shell test to seven digits; the centrepost-life numbers reproduce arithmetically from the frozen three-dimensional OpenMC fluence data (ENDF/B-VIII.0, seed 20260726). This paper is archived at doi:10.5281/zenodo.22645786 and its official version is at https://www.kronosfusionenergy.com/publications/supply-chain-and-fleet-buildability.html. No result depends on unpublished or proprietary data, and no economic quantity is reported.

Data availability tocsectionData availability The bill-of-materials masses, the enrichment anchors, the separative-work cascade, and the centrepost life/shield trade used for the figures are archived with the deposit at doi:10.5281/zenodo.22645786 and trace to the register [28] by the serial identifiers cited inline (SC-BR-1, SC-BR-2, SC-BR-5, ENV-A4). Cost content is excluded from the public deposit.

Competing interests tocsectionCompeting interests Provisional patent applications relating to aspects of this work have been filed.

tocsectionReferences

APPARATUS

Portfolio, People & Record

The intellectual-property estate, the people who built it, the limitations that gate it, and the sources it rests on.

1	4	40	27
GRANTED PATENT	2026 PROVISIONALS	TEAM MEMBERS	2022 PROVISIONALS

INTELLECTUAL PROPERTY

The patent portfolio

The estate spans a granted high-field magnet patent, pending utility and 2026 provisional filings that map to the two products, a digital-twin control provisional, a registered trademark application, and the original 2022 provisional family. Every patentable disclosure in the five-paper arXiv drop was protected **before** publication: the breeder and burner provisionals were filed 1–2 August, and a publication-gap omnibus filing the evening before the drop swept up the DEC, plasma-control, and REBCO-winding matter of the three otherwise-unprotected papers. Patent numbers and application serials are matters of public record; claim scope is summarised, not reproduced.

GRANTED & PENDING UTILITY

US 12,009,112	High-field tilted graded-REBCO magnet architecture (KRONO-002A) · *app. 17/878,550*	GRANTED
US 17/878,507	Core device / method (KRONO-001A) · *utility*	PENDING

2026 PROVISIONAL FILINGS — MAPPED TO THE PRODUCTS

64/124,209	Hyperion — spherical-tokamak tritium / helium-3 foundry · *breeder · filed Aug 2026*	FILED
64/124,220	Aegis / MetroVolt — synchrotron-cutoff, fuel-selection & plug-winding · *generator · filed Aug 2026*	FILED
64/115,167	KRONOS-CTRL digital-twin plant control · *provisional · filed Jul 2026*	FILED
64/005,440	Integrated spherical-tokamak fusion architecture · *early integrated-architecture filing · filed Mar 2026*	FILED
64/105,530	Negative-triangularity spherical-tokamak architecture · *foundational ST filing · filed Jul 2026*	FILED
64/128,097	Publication-gap omnibus — quasineutral two-species expander DEC · provenance-gated / latency-split plasma control · as-built high-field winding & conductor architecture · *filed 7 Aug 2026, the evening before the arXiv drop*	FILED

TRADEMARK & ORIGIN

FTK-98801894	Kronos Fusion Energy — trademark application	FILED
KR-2022-*	Original provisional family (KR-2022-00001 … 00027) · *27 filings, 2022*	PRIORITY

The narrow, defensible magnet novelty — the specific conductor and the digital-twin winding optimisation, not high-field REBCO as a category — is the commercial core that can earn ahead of any $Q > 1$ milestone, with markets in fusion magnet supply, MRI/NMR, accelerators, and proton therapy. The claim is scoped honestly: the high field is a *system field* result, not a stand-alone-coil record; the small-bore plug coil is structurally infeasible as a bare winding but resolved by a stress-managed structural shield (feasible-pending-FEA); and the winding-tape experiment returned a *null result*. The value is the method, not a field record.

THE TEAM

Founding partners, board, advisors & auditors

Kronos is built by a bench of advanced-fuel-fusion, high-field-magnet, direct-conversion, and materials specialists, with a board and operations team drawn from defense, national laboratories, and industry. Dates are shown as ranges; where a tenure has ended or is term-ending, the range says so.

FOUNDING PARTNERS — SCIENCE

Dr. Gerald Kulcinski
Co-Founder · Helium-3 & Advanced-Fuel Fusion
UW–Madison · 2023–Present

Dr. Carl Weggel
Chief Scientist / S.M.A.R.T. Design
MIT Alcator Program · 2022–Present

Dr. Robert J. Weggel
Magnetic Field Design
MIT Magnet Lab · 2022–Present

BOARD

Priyanca Ford
Founder & CEO · Executive Board
2022–Present

Bandel Carano
Finance / Strategy
Oak Investment Partners / Stanford · 2025–2026

Patrick Schweiger
Fusion Device Engineering
Oklo / CFS / TerraPower · 2025–Present

SCIENTIFIC ADVISORS

Dr. Steven O. Dean
Fusion Policy & History
DOE / Fusion Power Associates · 2025–Present

Dr. Patrick H. Diamond
Plasma Turbulence & Transport
UC San Diego · 2025–Present

Dr. Jack J. Dongarra
HPC & Numerical Algorithms
Turing Award · 2025–Present

Dr. Nasr M. Ghoniem
Chief Material Scientist
UCLA · 2025–Present

Dr. Siegfried Glenzer
Plasma Physics & Laser Fusion
Stanford / SLAC · 2022–Present

Dr. David A. Hammer
Pulsed-Power Fusion
Cornell · 2025–Present

Dr. Donald A. Spong
Plasma Theory & Confinement
ORNL · 2025–Present

Dr. Curtis Smith
Risk Assessment & Nuclear PRA
MIT / Idaho National Lab · 2025–Present

RADM (Ret.) David Goggins
Naval Engineering & Power-Plant Design
U.S. Navy · 2023–2026

Dr. Konstantin Batygin
Mathematician
Caltech · 2022–2025

Dr. Ruben Fair
Magnet Design / ITER Liaison
PPPL / Jefferson Lab · 2022–2025

Dr. Paul S. Weiss
Materials & Nanotechnology
UCLA · 2022–2025

SCIENTIFIC AUDITORS

Dr. Wilfred A. Cooper
Plasma Equilibrium Theory
EPFL / Swiss Plasma Center · 2025–Present

Dr. Ahmed Hassanein
Plasma–Material Interactions
Purdue / Argonne · 2025–Present

Dr. Patrick E. Hopkins
Extreme Thermal Materials
U. of Virginia · 2025–Present

Dr. Peter Hosemann
Materials Joining & Structural Integrity
UC Berkeley · 2025–Present

Dr. Travis W. Knight
Advanced Nuclear Fuels & Systems
U. of South Carolina · 2025–Present

Dr. Philippe Lebrun
Cryogenics & Magnet Cooling
CERN · 2025–Present

Dr. Nitendra Singh
Nuclear Safety & Fuel Cycle
ITER · 2025–Present

Dr. Guido Van Oost
Magnetic Confinement & Fusion Systems
Ghent University · 2025–Present

Dr. Gary S. Was
Radiation Materials & Structural Integrity
U. of Michigan · 2025–Present

Dr. Ray Sedwick
Direct Energy Conversion
U. of Maryland · 2025

OPERATIONS

Michael Laughlin
Chief Operating Officer
2022–Present

Martin Owens
Chief Strategy Officer
LANL / GE Hitachi · 2022–Present

MG (Ret.) Paul Pardew
Chief Contracting Officer
Army Contracting Command · 2022–Present

David Beck
Fusion Commercialization
U.S. Space Force · 2024–Present

Sushma Bhatia
Environmental & Legislative
Google · 2022–Present

Michael De Frenza
Technology Licensing
2023–Present

MG (Ret.) Robin L. Fontes
Cybersecurity & Defense
Army Cyber Command · 2022–Present

Vijay Gehani
Supply Chain & Components
INOX India · 2024–Present

Jon Michel Greenwood
IT & AI Infrastructure
Live Nation · 2023–Present

Brian C. O'Neill
National Security
CIA / ODNI · 2022–Present

Gen. (Ret.) Gustave F. Perna
DoD Liaison
Operation Warp Speed · 2022–2023

Andrea Romero
Marketing Lead
2022–Present

Legal counsel is retained; those roles are held on the internal roster and are not listed here.

SOURCES

References

1 B N Sorbom *et al*, ARC: a compact, high-field, fusion nuclear science facility and demonstration power plant with demountable magnets, *Fusion Eng. Des.* **100** 378 (2015). doi:10.1016/j.fusengdes.2015.07.008

2 A J Creely *et al*, Overview of the SPARC tokamak, *J. Plasma Phys.* **86** 865860502 (2020). doi:10.1017/S0022377820001257

3 J E Menard *et al*, Fusion nuclear science facilities and pilot plants based on the spherical tokamak, *Nucl. Fusion* **56** 106023 (2016). doi:10.1088/0029-5515/56/10/106023

4 J L MacManus-Driscoll and S C Wimbush, Processing and application of high-temperature superconducting coated conductors, *Nat. Rev. Mater.* **6** 587 (2021). doi:10.1038/s41578-021-00290-3

5 M E Austin *et al*, Achievement of reactor-relevant performance in negative triangularity shape in the DIII-D tokamak, *Phys. Rev. Lett.* **122** 115001 (2019). doi:10.1103/PhysRevLett.122.115001

6 A Marinoni, O Sauter and S Coda, A brief history of negative triangularity tokamak plasmas, *Rev. Mod. Plasma Phys.* **5** 6 (2021). doi:10.1007/s41614-021-00054-0

7 M Abdou *et al*, Physics and technology considerations for the deuterium–tritium fuel cycle and conditions for tritium fuel self sufficiency, *Nucl. Fusion* **61** 013001 (2021). doi:10.1088/1741-4326/abbf35

8 M Kovari, M Coleman, I Cristescu and R Smith, Tritium resources available for fusion reactors, *Nucl. Fusion* **58** 026010 (2018). doi:10.1088/1741-4326/aa9d25

9 F A Hern\'andez and P Pereslavtsev, First principles review of options for tritium breeder and neutron multiplier materials, *Fusion Eng. Des.* **137** 243 (2018). doi:10.1016/j.fusengdes.2018.09.014

10 M Abdou *et al*, Blanket/first wall challenges and required R&D on the pathway to DEMO, *Fusion Eng. Des.* **100** 2 (2015).

11 F A Hern\'andez *et al*, A new HCPB breeding blanket for the EU DEMO: evolution, rationale and preliminary performances, *Fusion Eng. Des.* **124** 882 (2017).

12 L V Boccaccini *et al*, Objectives and status of EUROfusion DEMO blanket studies, *Fusion Eng. Des.* **109–111** 1199 (2016).

13 G Federici *et al*, European DEMO design strategy and consequences for materials, *Nucl. Fusion* **57** 092002 (2017).

14 U Fischer *et al*, Neutronics requirements for a DEMO fusion power plant, *Fusion Eng. Des.* **98–99** 2134 (2015).

15 T Giegerich, K Battes, J C Schwenzer and C Day, Development of a viable route for lithium-6 supply of DEMO and future fusion power plants, *Fusion Eng. Des.* **149** 111339 (2019).

16 E A Symons, Lithium isotope separation: a review of possible techniques, *Separation Science and Technology* **20** 633 (1985).

17 A Molodyk *et al*, Development and large volume production of extremely high current density $YBa_2Cu_3O_7$ superconducting wires for fusion, *Sci. Rep.* **11** 2084 (2021). doi:10.1038/s41598-021-81559-z

18 Z S Hartwig *et al*, VIPER: an industrially scalable high-current high-temperature superconductor cable, *Supercond. Sci. Technol.* **33** 11LT01 (2020). doi:10.1088/1361-6668/abb8c0

19 S Hahn *et al*, 45.5-tesla direct-current magnetic field generated with a high-temperature superconducting magnet, *Nature* **570** 496 (2019). doi:10.1038/s41586-019-1293-1

20 P K Romano, N E Horelik, B R Herman, A G Nelson, B Forget and K Smith, OpenMC: a state-of-the-art Monte Carlo code for research and development, *Ann. Nucl. Energy* **82** 90 (2015). doi:10.1016/j.anucene.2014.07.048

21 D A Brown *et al*, ENDF/B-VIII.0: the 8th major release of the nuclear reaction data library, *Nucl. Data Sheets* **148** 1 (2018). doi:10.1016/j.nds.2018.02.001

22 P Bruzzone *et al*, High temperature superconductors for fusion magnets, *Nucl. Fusion* **58** 103001 (2018).

23 L M Giancarli *et al*, Overview of the ITER TBM Program, *Fusion Eng. Des.* **87** 395 (2012).

24 D G Whyte, J Minervini, B LaBombard *et al*, Smaller & sooner: exploiting high magnetic fields from new superconductors for a more attractive fusion energy development path, *J. Fusion Energy* **35** 41 (2016).

COLOPHON

How this document was made

The Kronos Fleet — Combined Editorial, 2026 is set in **Fraunces** (display), **Gelasio** (text), and **IBM Plex Mono** (data & equations), carried forward from the Kronos editorial design system.

The figures are rendered at 300 dpi from the deposited generator scripts; the document is composed as a single self-contained file with embedded fonts and imagery, paginated to US Letter, and rendered to PDF through a headless Chromium engine in matched light and dark editions.

Every headline quantity carries an evidence class; withdrawn and restated values are marked as such. Nothing herein is frozen beyond the founder-approved Tier-A set.

Explore it live — turn the interactive 3-D model, run the deposited solvers in the physics validator, and watch the companion film series.

LEGAL NOTICE

Notice, status, and distribution

Conceptual design & simulation study. This document reports a conceptual design and simulation study. It is not a construction commitment, a safety-analysis report, a regulatory filing, or an offer of securities. Forward-looking statements — schedules, costs, market sizes, and performance — are estimates subject to the limitations set out in the Simulations part and may change.

Numbers and their classes. Quantities are reported with evidence classes and case labels; modelled, assumed, and requirement-class values are identified as such and are not to be quoted without their labels.

Public edition. This edition carries the physics and design only; all financial, funding, and defense-commercial content has been removed for public distribution. The scientific text corresponds to the arXiv and journal submissions.

THE 2026 KRONOS SERIES

One programme, many papers

This editorial is one paper in the Kronos 2026 series — a real fusion company's complete, reproducible physics record for a spherical-tokamak breeder and its low-neutron D–^{3}He tandem-mirror burners. Every headline number is a frozen anchor in the Physics De-Risking Register.

Explore the whole programme: the De-Risking Register, the interactive 3-D model, and the physics validator.

KRONOS FUSION ENERGY

Critical-Materials Buildability for a Spherical-Tokamak Breeder Fleet: Bottleneck Ranking of Li-6 Enrichment, Beryllium Fabrication and REBCO Tape Supply

A real fusion company building real machines. Explore the science, live.

Zenodo · doi:10.5281/zenodo.22645786

Read on kronosfusionenergy.com

The Physics De-Risking Register